APL Materials

Resonant dielectric metasurfaces in strong optical fields

Cite as: APL Mater. **9**, 060701 (2021); https://doi.org/10.1063/5.0048937
Submitted: 28 February 2021 • Accepted: 12 May 2021 • Published Online: 25 May 2021

Varvara Zubyuk, Luca Carletti, Maxim Shcherbakov, et al.

Resonant dielectric metasurfaces in strong optical fields

Cite as: APL Mater. 9, 060701 (2021); doi: 10.1063/5.0048937
Submitted: 28 February 2021 • Accepted: 12 May 2021 •
Published Online: 25 May 2021

Varvara Zubyuk,[1] Luca Carletti,[2,a)] Maxim Shcherbakov,[1,3,a)] and Sergey Kruk[4,5,a)]

AFFILIATIONS

[1] Faculty of Physics, Lomonosov Moscow State University, Moscow 119991, Russia
[2] Department of Information Engineering and National Institute of Optics (CNR-INO), University of Brescia, Brescia 25123, Italy
[3] School of Applied and Engineering Physics, Cornell University, Ithaca, New York 14853, USA
[4] Department of Physics, Paderborn University, 33098 Paderborn, Germany
[5] Nonlinear Physics Centre, Research School of Physics, Australian National University, Canberra ACT 2601, Australia

[a)] **Authors to whom correspondence should be addressed:** luca.carletti@unibs.it, mrs356@cornell.edu, and sergey.kruk@outlook.com

ABSTRACT

Optical materials are undergoing revolutionary transformations driven by nanotechnology. Our ability to engineer structures at a scale smaller than the wavelength of light enables new properties and functionalities otherwise not available in natural bulk optical materials. A class of such components—dielectric metasurfaces—employs two-dimensional arrays of designer resonant nanoscale elements whose optical response is defined by their geometry. While *linear* regimes of interactions between dielectric metasurfaces and moderately intense light have already formed a mature field of applied research and engineering, new frontiers are being actively explored in the *nonlinear* optical regime describing interactions of metasurfaces with strong optical fields. In this Research Update, we cover the most recent progress along with several directions of research within the field of nonlinear optics of dielectric metasurfaces. Specifically, we review approaches to design and fabricate metasurfaces with high local field enhancements that facilitate nonlinear light–matter interactions, outline nonlinearity-enabled functionalities of dielectric metasurfaces, explore resonant metasurfaces in the strong-field non-perturbative regime, and discuss the implications of the time-variant refractive index in metasurfaces that interact with strong optical fields produced by laser pulses.

I. INTRODUCTION

A sufficiently intense beam of light interacting with a material can temporarily modify the optical properties of the material, with the magnitude of such modification being *nonlinearly* proportional to the amplitude of the electromagnetic field of the incident light. Examples of nonlinear light–matter interactions are sketched in Figs. 1(a)–1(c). Nonlinear regimes of light–matter interactions open a plethora of new optical phenomena, such as the alternation of the frequency of the output light, multiphoton absorption, and strong self-action effects, among others. Usually, nonlinear interactions are weak and become observable only after light travels through a material over relatively long distances consisting of many thousands of wavelengths. Many conventional nonlinear optical systems typically require the combination of bulk volumes of a material with a confining cavity, which increases the photon lifetime, thus strengthening light–matter interactions. However, the recent developments of resonant nanostructures facilitating strong light concentrations opened the path toward efficient nonlinear processes on a scale smaller than the wavelength of light.

In the recent past, many demonstrations were performed with engineered metallic nanoparticles.[1–4] Metals were an attractive choice as they exhibit extremely high intrinsic nonlinearities. In addition, the support of plasmon resonances allows for dramatic light confinement and local intensity enhancement near plasmonic hot spots. However, the overall efficiency of the nonlinear processes in plasmonic nanostructures remained low,[5,6] limited by ohmic losses, small mode volumes confined within metal surfaces, and low laser damage thresholds.

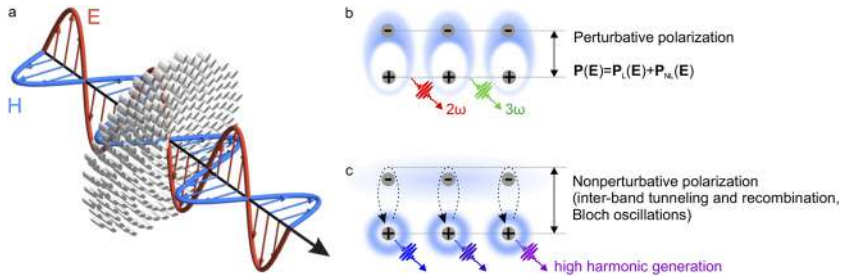

FIG. 1. Materials in strong optical fields. (a) Representation of an electromagnetic wave passing through a material patterned at a subwavelength scale. A sufficiently strong optical field induces several types of nonlinear light–matter interactions. In this Research Update, we will be primarily interested in the following two types of interactions. Moderately strong fields may induce material polarization **P**(**E**) consisting of linear [$\mathbf{P}_L(\mathbf{E})$] and nonlinear [$\mathbf{P}_{NL}(\mathbf{E})$] components (b). Extremely strong fields may cause generation and subsequent recollision of free electrons and holes driven by the incident electromagnetic field (c).

All-dielectric nanostructures have recently been suggested as an alternative way to enhance the nonlinear efficiency beyond the limits associated with plasmonics. High refractive index nanoparticles can support multiple different types of optical modes, including optically induced magnetic dipole resonances, higher-order multipoles, and composite resonances.[7–10] High field enhancements near the magnetic dipole modes and composite resonances increase the efficiency of nonlinear processes by orders of magnitude compared to their plasmonic counterparts. Low or negligible absorption at the pump wavelength allows the electric field to penetrate in nanostructures and grant access to the nonlinear response of the whole volume of its material. Another relevant consequence of transparency at the pump wavelength is the high laser damage threshold of all-dielectric nanoresonators.

Material platforms employed in the field of nonlinear metasurfaces include high refractive index dielectric and semiconductor materials, such as Si and Ge[11–13] [high values of (3) nonlinear susceptibility tensor], and the group of III–V semiconductors, such as GaAs and GaP[14–16] [high values of (2) nonlinear susceptibility tensor], among others. Lithium niobate,[17–19] titanium dioxide,[20] and barium titanate[21] were employed for nonlinear metasurfaces in spectral ranges down to ultraviolet (UV) wavelengths. Novel emerging classes of materials are actively explored, including epsilon-near-zero materials, such as ITO,[22–24] phase-change materials,[25] and 2D materials, such as WS_2,[26] GaSe,[27] and multi-quantum-well heterostructures.[28,29] Recently, liquid-phase dielectrics have also been explored as metasurface materials.[30]

Engineered optical resonances play a central role in the field of nanoscale nonlinear optics. Resonant effects can intensify electromagnetic fields within nonlinear materials by orders of magnitude, thus dramatically enhancing the efficiency of nonlinear light–matter interactions.[31,32]

II. ENHANCEMENT OF NONLINEAR LIGHT–MATTER INTERACTIONS AT THE NANOSCALE

In the recent past, several different strategies have been explored for the enhancement of nonlinear light–matter interactions in metasurfaces via engineered resonances. Here, we overview some of the approaches. We attempt to provide, where applicable, a figure of merit for efficiencies of nonlinear light–matter interactions that we discuss below. We note, however, inherent limitations of any quantitative figure of merit as the reviewed experiments vary by multiple parameters (laser source pulse duration, repetition rate, peak, and average power). To this end, we predominantly focus on nonlinear frequency doubling and frequency tripling effects [second-harmonic generation (SHG) and third-harmonic generation (THG)], for which multiple experiments have been conducted by several groups. We evaluate the strength of the nonlinear interaction in the following form of the ratio of the peak powers of the pump and generated harmonic for second-harmonic and third-harmonic generations, respectively:

$$\beta = \frac{P_{SH}^{p}}{\left(P_{FF}^{p}\right)^{2}}, \quad \gamma = \frac{P_{TH}^{p}}{\left(P_{FF}^{p}\right)^{3}}.$$

Here, P_{FF}^{p} is the incident peak power of the pump beam at the fundamental frequency (FF) and P_{SH}^{p} and P_{TH}^{p} are the peak powers of SHG and THG, respectively. The coefficients β and γ have units of W^{-1} and W^{-2}, respectively, and can be useful as they mitigate some dependencies on the exact parameters of a particular excitation laser source.

Nonlinear generation of second and third optical harmonics in dielectric nanostructures has been demonstrated at the level of both isolated nanoresonators and their 2D layouts—metasurfaces. We, therefore, discuss the resonant characteristics of both the individual elements and the collective effects induced by the lattice and the coupling between adjacent elements. The enhancement of nonlinear phenomena is determined by different factors: the quality factor (Q-factor) of the resonance at the pump wavelength, the Q-factor of the harmonic resonance, the spatial and spectral overlap between pump and harmonic resonances, and the efficiency of the coupling of the pump beam to the resonator. Since second- and third-order nonlinear light–matter interactions depend correspondingly on the second and third powers of the electric field inside the nonlinear material, a prime approach to enhance the efficiency of these phenomena is to enhance the quality factor of the resonance and the pump mode. Below, we briefly outline several approaches for engineering optical resonances in subwavelength dielectric structures.

A. Mie resonances

Mie resonances were introduced as the exact Mie solutions of Maxwell's equations describing light interactions with spherical

particles.[33,34] In a more recent past, numerical approaches allowed application of the concept of Mie resonances to small objects of arbitrary shapes. Mie resonances have attracted attention because they can support both electric and magnetic type resonances of comparable strengths.[7,31,35,36] Typically, individual low-order Mie resonances have quality factors below ten, and some of the best demonstrations of SHG and THG based on the magnetic dipole resonant pump yield $\beta = 2 \times 10^{-8}$ W^{-1}[37] and $\gamma = 2.6 \times 10^{-14}$ W^{-2},[38] respectively. Nevertheless, the fact that multiple resonances can interfere with one another opens new pathways to enhance the mode Q-factor in nanostructures.

B. Toroidal moments

Toroidal multipoles represent another example of fundamental solutions of Maxwell's equations. While Mie resonances are conventionally calculated from the expansion of electromagnetic potentials and charges into a series of multipoles, toroidal multipoles can be derived via decomposition of the momentum tensors.[39,40] The electromagnetic field produced by a toroidal dipole moment resembles the field produced by an electric current wire wrapped into a coil, with the coil being further arranged into a torus shape, which gives rise to an effective magnetic current loop. The concept of toroidal resonances has also been generalized to higher-order toroidal moments of both electric and magnetic nature. Toroidal moments were introduced to metamaterials and metasurfaces first in microwaves.[41] Later on, optical all-dielectric metasurfaces supporting toroidal moments have been proposed theoretically[42–44] and demonstrated experimentally.[45,46] The enhancement of nonlinear light–matter interactions by toroidal moments has been studied in optics in plasmonic metasurfaces[47] and suggested theoretically in all-dielectric designs.[42]

C. Isolated nanoparticles: Anapole modes

Toroidal moments of light gave birth to the concept of optical anapoles. The first-order anapole excitation is achieved when an electric dipole and toroidal dipole moments of the nanoparticle have the same or similar amplitude and are out-of-phase.[48] The electric field radiated by a toroidal dipole moment matches the one that is radiated by an electric dipole, and thus, if the previous condition is satisfied, the radiation patterns of these two multipoles interfere destructively, canceling the output channels of radiation leakage. This leads to a non-trivial radiationless current distribution in the nanoparticle. In general, this interference mechanism is not enough to suppress outward radiation from the nanoparticle: for external excitation (e.g., illuminating the nanoparticle with a laser beam), magnetic quadrupole and electric octupole moments that accompany the toroidal moment remain radiative. Nevertheless, this condition leads to an enhancement of the field intensity inside the nanoparticle. Anapole modes were demonstrated to reach Q-factors estimated around 10–50.[49–52] The quality factors of anapole resonators are mainly limited by the existence of other multipoles within the same spectral range. One technique to enhance the electric field confinement by anapoles employed hybrid dielectric-metallic nanostructures.[53,54] A nanodisk supporting the anapole condition is surrounded by a gold ring possessing a plasmonic resonance at the same wavelength. Another recently proposed technique to increase the Q-factor of anapole resonances utilized a metallic substrate underneath the nanoresonator. The metallic plane, to a first approximation, created a mirror image of anapole modes, allowing it to achieve destructive interference in the radiation pattern of parasitic multipoles, and thus improving mode confinement and yielding Q ~ 50 in Ref. 49. This method enabled the demonstration of THG from Si nanodisks with $\gamma = 3.9 \times 10^{-7}$ W^{-2} [see Fig. 2(c)].

D. Isolated nanoparticles: Bound states in the continuum

One more promising approach to engineer high-Q modes in single nanoresonators has recently emerged, inspired by the physics of bound states in the continuum (BIC).[55] The BIC originates from the complete destructive interference of two or more waves, effectively suppressing all radiative losses. This requires infinitely large structures or materials with either zero or infinite permittivity. Nevertheless, dielectric nanoparticles host a wide variety of leaky optical modes that can be geometrically tuned. When leaky modes with similar far-field profiles are found at similar frequencies, they can eventually undergo a strong coupling regime featuring avoided resonance crossing. This results in one of the two leaky modes exhibiting an extraordinarily high Q-factor for isolated nanoparticles. Such a condition is called accidental BIC or quasi-BIC,[59] owing to the similar physics with the Friedrich–Wingten BIC.[60] The Q-factor that such structures can achieve at near-infrared frequencies is on the order of $(1-3) \times 10^2$.[14,55,61,62] Recent experiments traced the evolution of scattering spectra of isolated nanoparticles vs their geometrical parameter demonstrating the quasi-BIC regime for optimal parameter settings.[63] The scattering spectra are fundamentally related to the dynamics of a Fano resonance. It was shown that the collapse of the leaky mode into the quasi-BIC state is associated with a divergence of a Fano line shape parameter ($q \to \infty$). The high Q-factor of BICs in nanoparticles is very promising for nonlinear applications. After initial theoretical predictions for both SHG[62] and THG[61] with BIC systems, experimental demonstration of SHG in GaAs nanodisks on an engineered substrate enabled $\beta = 1.3 \times 10^{-6}$ W^{-1},[14] which is illustrated in Figs. 2(a) and 2(b).

E. Collective modes in metasurfaces: Fano resonances

The Fano resonance occurs when a dark (high-Q) mode is coupled via near-field to a bright (low-Q) mode. This results in a reflectance or transmittance spectrum exhibiting a Fano line shape.[64,65] As the dark mode is excited via the near-field coupling, the achievable Q-factor can be very high. In Ref. 56, a disk-bar configuration was adapted for THG. The Q-factor of the metasurfaces at the pump wavelength was Q = 466, and the measured THG nonlinear coefficient was $\gamma = 1.9 \times 10^{-13}$ W^{-2} [see Fig. 2(d)].

F. Collective modes in metasurfaces: Symmetry-protected bound states in the continuum

In systems possessing reflection or rotational symmetries, optical modes of different symmetry classes decouple. In subwavelength metasurfaces, the only radiative channels are plane waves propagating in the normal direction with respect to the

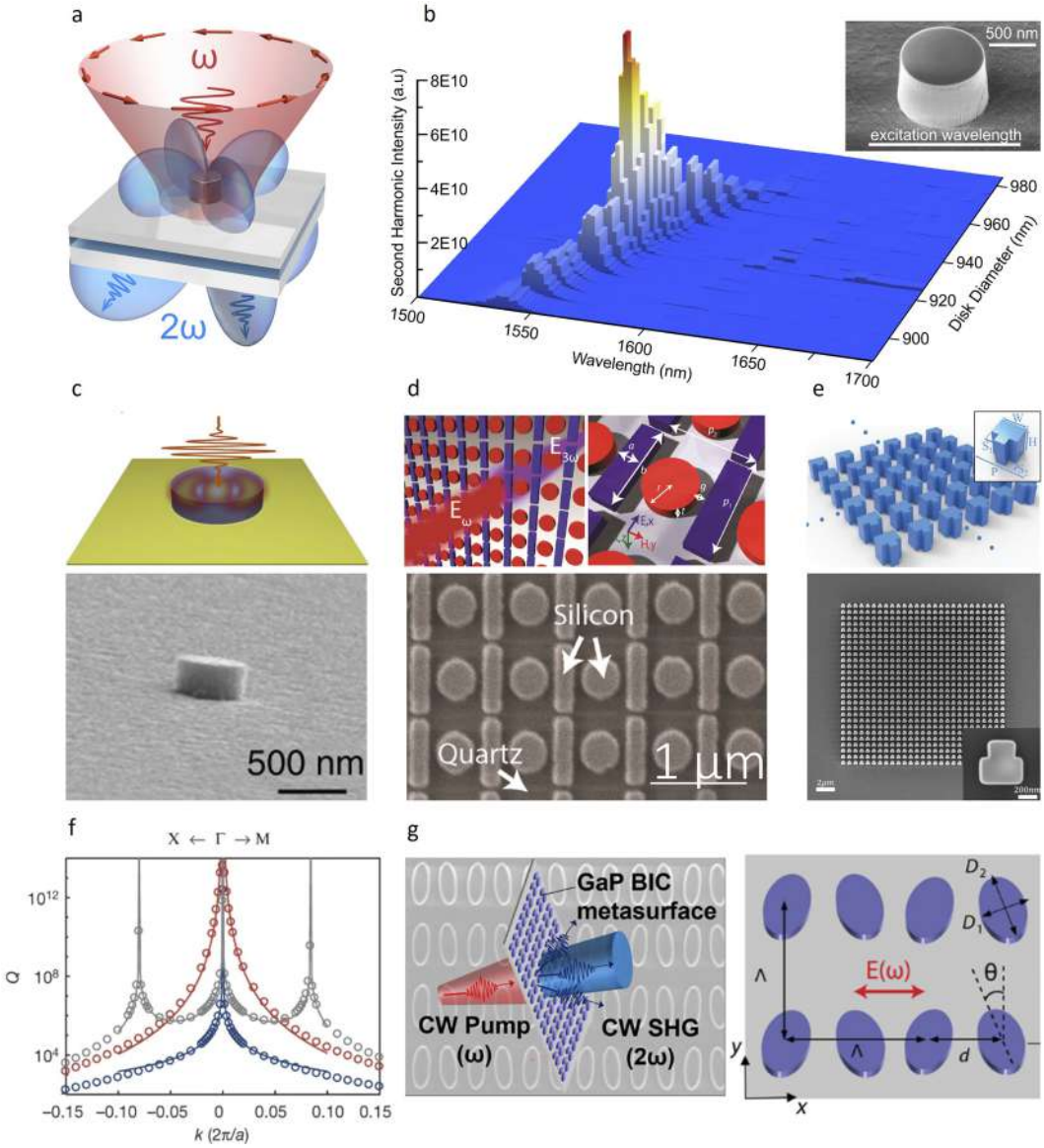

FIG. 2. Dielectric nanostructures for enhancement of interactions between materials and optical fields. (a) Concept image of a subwavelength resonator for nonlinear second-harmonic generation. A portion of the incident beam at frequency ω (red) gets converted into frequency 2ω (blue). (b) Inset: scanning electron micrograph of the AlGaAs subwavelength resonator with a Q-factor of 188 facilitated by a quasi-BIC resonance. The plot visualizes the measured intensity of second-harmonic generation in such AlGaAs resonators as a function of resonator size and the excitation wavelength. Once the resonant conditions are met, the efficiency of the nonlinear optical process increases by several orders of magnitude.[14] (c) Anapole in a resonator-on-PEC-surface system. Top: schematic illustration of the field distribution of an anapole resonator on a PEC (perfect electric conducting) substrate. Bottom: scanning electron micrograph of the fabricated resonator on a mirror.[49] (d) Fano-resonant metasurface. Bottom: scanning electron micrograph image of the fabricated metasurface.[56] (e) Quasi-BIC in a metasurface. Bottom: scanning electron micrograph image of the fabricated device.[57] (f) High-Q modes merging.[51] (g) Harmonic generation from a metasurface in the continuous-wave (CW) regime. High-Q modes in quasi-BIC GaP metasurfaces enable the sufficient local field enhancement to observe SHG under CW excitations. The schematic of the quasi-BIC GaP metasurfaces (right).[58]

metasurface plane. In this case, the electric and magnetic field vectors are odd upon C_2 rotations; thus, modes that are even with respect to the same transformation are completely decoupled from the continuum of radiation and form a BIC. Such BICs have recently been thoroughly investigated in metasurfaces.[59] The Q-factor of BICs in its pure mathematical sense is infinite; thus, excitation of these modes is forbidden. Nevertheless, maintaining an excitation beam that normally impinges on the metasurface, once the symmetry of the unit cell is broken, coupling of free-space radiation can be achieved. Asymmetry limits the

Q-factor to a finite value opening radiation channels and converting the resonance in a so-called "quasi-BIC." Remarkably, the exact value of the Q-factor can be fine-tuned by the level of introduced asymmetry.[66] In particular, one can define an asymmetry parameter, α, and in the limit of small perturbations, the Q-factor is shown to scale as $1/\alpha^2$. This approach has been adapted for both SHG,[67] demonstrating a $\beta = 9.6 \times 10^{-8}$ W^{-1}, and THG,[68] demonstrating a $\gamma = 1.5 \times 10^{-14}$ W^{-2}. The Q-factor of the two works was Q = 500 for the SHG metasurface and Q = 100 for the THG metasurface. More recently, in Ref. 57, the authors proposed a symmetric approach for breaking the symmetry of the meta-atom that enabled a significant improvement of the Q-factor 1.8×10^4. Such a high-Q mode was used as a pump for THG, yielding a nonlinear coefficient of $\gamma = 1.4 \times 10^{-8}$ W^{-2} [see Fig. 2(e)].

A remarkable approach was recently demonstrated by Jin *et al.* in Ref. 51. Researchers studied a nanopatterned silicon membrane supporting multiple symmetry-protected BICs. By judiciously designing geometrical parameters of the nanopattern, Jin and co-authors were able to overlap multiple bound states in the continuum in the momentum space. As a result, an order of magnitude increase in the Q-factor was measured experimentally under the condition of merged BICs reaching a Q-factor of 4.9×10^5 [see Fig. 2(f)]. Such super-BIC resonances may find their applications in nonlinear optics as well as pave the way toward a general strategy of increasing quality factors of nanostructures via novel interference scenarios of several resonant modes.

G. Machine learning

Theoretical models, such as anapoles, Fano resonances, and BICs, provide guidelines for efficient designs of nonlinear nanostructures. However, determination of final details of nanostructure's geometries typically relies on iterative 3D numerical full-wave simulations, such as finite-element method (FEM), finite-difference time-domain (FDTD) method, and others, which are computationally demanding, especially for solving nonlinear problems. To reduce the number of trial-and-error iterations of full-wave simulations, various optimization strategies are often implemented, such as genetic algorithms and gradient descent methods.[69–71]

Radically different emerging approaches for the design of subwavelength photonic structures are based on machine learning.[72–74] Among the various machine learning methods, deep neural network (DNN) techniques have demonstrated great potential. DNNs usually contain multiple hidden layers that provide a sufficient number of units, which can be used to represent complicated functions to uncover hidden relations between variables, such as between nanophotonic structure geometries and their electromagnetic responses.[75–78] This makes DNN-based techniques promising for solving the inverse problem in nanophotonics: to predict the geometry with given properties, such as to predict design parameters of a metasurface hosting a high-Q resonance. To this end, the DNN-based methods have been demonstrated to predict accurately amplitude[72,79–82] and phase[80,83–85] spectra of metasurfaces. Employment of DNNs for nonlinear nanophotonics, in particular, for the enhancement of the efficiencies of light–matter interactions at the nanoscale sounds particularly appealing, given the complexity of the wide range of nonlinear optical interactions.

H. From pulsed to continuous-wave nonlinear nanophotonics

Due to the intrinsically low magnitude of the optical nonlinear response of the materials, nonlinear nanophotonics is dominated by interactions between matter and short laser pulses with typical durations on the order of tens and hundreds of femtoseconds. Such short pulses may reach high levels of peak power, thus enhancing nonlinear light–matter interactions while minimizing parasitic effects such as heating and free-carrier dispersion. However, as the Q-factor of the nanoresonators increases, extreme field intensities can be achieved even from more modest pump power levels. Moreover, the spectral overlap between the bandwidth of the pump and the resonance plays a key role in the enhancement of conversion efficiencies.[86] Thus, in view of the most recent progress in resonant nanophotonics, nonlinear light–matter interactions between nanostructures and continuous-wave (CW) lasers with much lower peak powers compared to their pulsed counterparts may be within reach. This road has already been followed in other nonlinear optics research areas such as photonic crystals and microcavities. In a recent paper, gallium phosphide metasurfaces with Q-factors varying from Q = 60 to Q = 2×10^3 have been used in both femtosecond and CW regimes[58] [see Fig. 2(g)]. It was shown that the increase in the Q-factor in the CW regime consistently improved the nonlinear response of the structure. In contrast, in the femtosecond regime, the SHG conversion efficiency saturated as a function of the Q-factor after the bandwidth of the resonance has become comparable to the bandwidth of the excitation pulse.

III. FUNCTIONALITIES ENABLED BY NONLINEAR LIGHT–MATTER INTERACTIONS

Nonlinear light–matter interactions hold promise to expand the range of application of metasurfaces as nonlinearity-enabled properties and functionalities go beyond the limitations of linear optics. Here, we discuss several recent demonstrations of metasurfaces with functionalities derived from their nonlinear optical response.

A. Nonlinear wavefront control

Several approaches for engineering the wavefront of parametric waves have been suggested and demonstrated experimentally. The methods rely on full control over the phase of generated light within the $0–2\pi$ range, thus allowing wavefront shaping.

A method that relies on *resonant phase accumulation* was suggested and demonstrated in Refs. 11, 87, and 88. The approach relied on the generalized Huygens' principle in nonlinear optics. This method was used to demonstrate experimentally a nonlinear metasurface beam deflector, a vortex beam generator[11] [see Fig. 3(a)], a nonlinear lens[87] [see Fig. 3(b)], and nonlinear holograms.[88]

Another demonstrated approach to control the wavefront of parametric waves based on geometric phase generalized for nonlinear light–matter interactions.[89–91] Geometric phase metasurfaces, also known as Pancharatnam–Berry phase metasurfaces, achieve a continuous phase change linked to a rotation angle of a low-symmetry nanoresonator. In the nonlinear case of the generation of optical harmonics, the geometric phase approach connects the rotation angle of a single nanoresonator to the phase shift at the

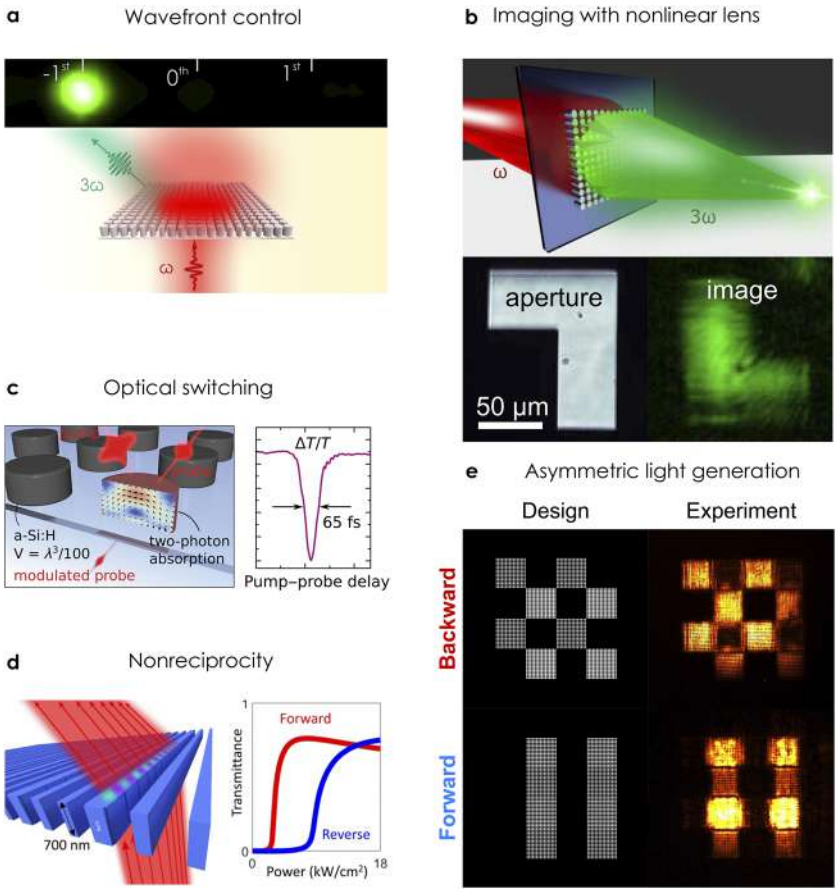

FIG. 3. Functional nonlinear metasurfaces. (a) Silicon metasurface controlling wavefront of the generated third-harmonic optical beam.[11] (b) Imaging of an L-shape aperture through a nonlinear metasurface lens.[87] Infrared light is transmitted through an aperture, and a visible image is formed by a metasurface generating third harmonic. (c) All-optical ultrafast switching in the silicon metasurface at the magnetic dipole Mie resonance.[93] (d) The theoretical concept of nonreciprocal forward/backward transmission in the nonlinear metasurface.[94] (e) Generated independent visible images in transmission for the opposite directions of infrared illumination by a nonlinear metasurface.[95]

generated harmonic. The nonlinear geometric phase was adopted in the dielectric metasurface from their plasmonic counterparts.[92] Using this method, nonlinear beam deflectors[89] and holograms[90,91] have been demonstrated in all-dielectric metasurfaces for both second-[89] and third-harmonic generation processes.[90,91]

B. Nonlinear lenses

The advancement in all-dielectric metasurfaces led to the development of flat lenses of submicrometer thickness. The concept has been transferred to the field of nonlinear metasurfaces, while nonlinear focusing and holography[96] and second-harmonic imaging[97] have been demonstrated first in plasmonic metasurfaces. More recently, all-dielectric nonlinear metalenses were demonstrated for focusing nonlinear imaging of objects as well as higher-order correlations of light from objects.[87] Interestingly, the wavefront control by nonlinear metasurface lenses was not grasped by conventional lens equations routinely used in linear optics, and modified nonlinear lens equations were suggested phenomenologically. Moreover, since the superposition principle of waves does not hold in the regime of nonlinear optics, such lenses were also demonstrating image formations accompanied by the autocorrelation function of the order of optical harmonics, thus carrying information about the coherence of light.

C. Optical switching and ultrafast tuning

Nonlinear metasurfaces have also been suggested as ultracompact optical switches. Several nonlinear optical processes have been applied in proof-of-concept demonstrations, including resonantly enhanced nonlinear absorption in silicon[93] [see Fig. 3(c)], nonlinear change in a refractive index at low optical power in chalcogenide glasses,[98] injection of free carriers,[99] and nonlinear absorption saturation[100] in direct bandgap semiconductors, such as GaAs, which were employed for metasurface-based switches.

D. Nonreciprocity and optical isolation

Optical nonreciprocity is the enabling property for several key functionalities in photonics, including optical isolation. The majority of optical systems are reciprocal, and nonreciprocity may be achieved in only a few conceptual pathways, one of which relies on nonlinear light–matter interactions.

Several theoretical proposals on achieving optical nonreciprocity in dielectric metasurfaces have been made recently for a different design starting from single-layer silicon structures[94] [see Fig. 3(d)] and then two-layer structures,[101] which due to Kerr nonlinearities of the material may be employed to realize a diode-like functionality in nanoscale optics. A theoretical proposal of an optical resonator made

from Si and ITO was suggested in Ref. 102. The design exploited optical nonlinearities of ITO in its epsilon-near-zero-regime,[103] suggesting nonreciprocal far-field radiation patterns.

E. Asymmetric control of light

Closely related to nonlinearity-induced nonreciprocity are processes of asymmetric frequency conversion and mixing in nonlinear nanoresonators and metasurfaces. Plasmonic designs with asymmetric nonlinear responses have been explored in the past theoretically[104,105] and experimentally.[106] Recently, all-dielectric translucent metasurfaces have been demonstrated that produced images in the visible spectral range via third-harmonic generation when illuminated by infrared radiation[95] [see Fig. 3(e)]. By design, the metasurfaces generated completely independent images for the opposite directions of illumination. This has been achieved via engineered bi-anisotropic coupling between electric and magnetic Mie resonances supported by the metasurfaces.

IV. HIGH OPTICAL HARMONIC GENERATION AND NON-PERTURBATIVE NONLINEAR REGIMES

Nonlinear optics of dielectric metasurfaces was originally dominated by second- and third-order nonlinear processes such as SHG and THG, examples of which were discussed above. These nonlinear processes are conventionally described within a *perturbative* framework, that is, assuming that the nonlinear component of material polarization is only a small perturbation to its linear counterpart. However, sufficiently intense optical excitations can bring materials beyond the boundaries of the perturbative approximation.

One of the most exciting outcomes of intense-field light–matter interactions is the effect of high-harmonic generation (HHG). HHG was observed in the decades following the development of the first lasers. Some of the milestone observations were the generation of optical harmonics up to the 11th order in gas plasma in 1977[107] [see Fig. 4(a)] and 33rd harmonic generation in 1988.[108] The physics of high-harmonic generation differs fundamentally from that of typical lower-order nonlinear processes, such as second- and third-harmonic generation. One consequence of the perturbative approximation is the scaling law of intensities of optical harmonics as $I_{n\omega} \propto I_{\omega}^{n}$, where I_{ω} is the intensity of the pump beam and $I_{n\omega}$ is the intensity of the n-th harmonic beam. This becomes inapplicable for descriptions of high-harmonic generation processes. One of the remarkable features of HHG is that the intensity of harmonics tends to a plateau, thus deviating strongly from the predictions of the perturbative model. Another striking difference is that HHG generation exhibits a cutoff frequency after which no harmonics can be observed.

The high-harmonic generation that was first studied in gasses and plasma could be commonly described with the *three-step recollision model*[109,110] within a framework of the strong-field approximation.[111] At the first step, an atomic gas undergoes ionization via the quantum tunneling mechanism upon optical excitation. During the second step, the ionized free electron is accelerated by the oscillating optical field initially from and then toward the parenting ion. At the final third step, the electron recollides with the ion. High-harmonic generation in atomic gases and plasma has been studied for decades, which has led to its applications in extreme-UV light sources,[112] generation of ultra-short light pulses,[113] and diagnostics techniques at atomic and molecular levels, such as probing of molecular orbitals.[114] Gas-phase HHG, however, involves expensive vacuum setups and complicated methods to confine the source gas within the interaction volume, thus limiting its applicability. More recently, HHG from solids has been demonstrated[115] [see Fig. 4(b)], revealing rich new physics[116] and offering systems with more compact form factors. Bulk solids, thin films,[117] and 2D materials[118,119] have been studied. Processes of HHG from solids were found to contradict predictions of both the perturbative theory of nonlinear optics and the three-step recollision model within the strong-filed approximation used to describe HHG in gases. Although details of the solid-state HHG mechanism remain a topic for debate,[116] the major differences with gas-state HHG originate from the high density of solids, leading typically to significant overlap of neighboring atomic orbitals. Another significant difference of solid-state systems is that due to their high density, the electron has a chance of recombining not with its parenting core but a neighboring core. Finally, the intensity scaling law of HHG as a function of pump intensity may be linear[115] in striking difference with the quadratic behavior typically observed in gas-phase HHG. Various approaches toward the detailed descriptions of the solid-state HHG can be found in Ref. 116 and references therein. Links between HHG from gases and solids have been studied recently[120] and remain an area of active research.

A. HHG in dielectric subwavelength structures and metasurfaces

Solid-state platforms allowed HHG to enter the realm of nanoscience, and several pathways to nanoscale HHG have been explored, including plasmonic nanostructures[124] as well as all-dielectric Fano-resonant metasurfaces[121] and gratings.[127] Some of the first experiments on HHG in subwavelength structures were conducted using plasmonic materials. Vampa *et al.* employed an array of gold nanoantennas to enhance optical harmonic generation in the underlying silicon substrate.[124] They observed up to ninth order harmonic generation and were able to achieve ten times overall enhancement of the harmonic generation intensity and estimated a 10^3–10^4 times enhancement in optical hot spots created by the antennas. Han *et al.* employed arrays of hybrid gold-sapphire truncated nanocones to generate harmonics up to 13th order in the extreme-UV spectral region at wavelengths as short as 60 nm.[122] The all-dielectric design further mitigated limitations of metallic nanostructures, such as relatively low laser damage threshold and absorption losses. Liu *et al.* demonstrated generation of optical harmonics up to 11th order in a silicon metasurface[121] that facilitates a sharp resonance mode that is associated with an optical analog of electromagnetically induced transparency. A similar design was conceptualized earlier for third-harmonic generation[56] and described in terms of Fano resonances. This leads to a multifold enhancement of optical fields inside silicon resonant elements. Zograf *et al.* demonstrated the generation of up to 11th optical harmonics in dielectric metasurfaces hosting optical modes associated with bound states in the continuum.[123] A set of metasurface hosting detuned quasi-BIC modes was developed, which allowed tracing transitions between perturbative and non-perturbative nonlinear regimes experimentally. The use of non-centrosymmetric materials,

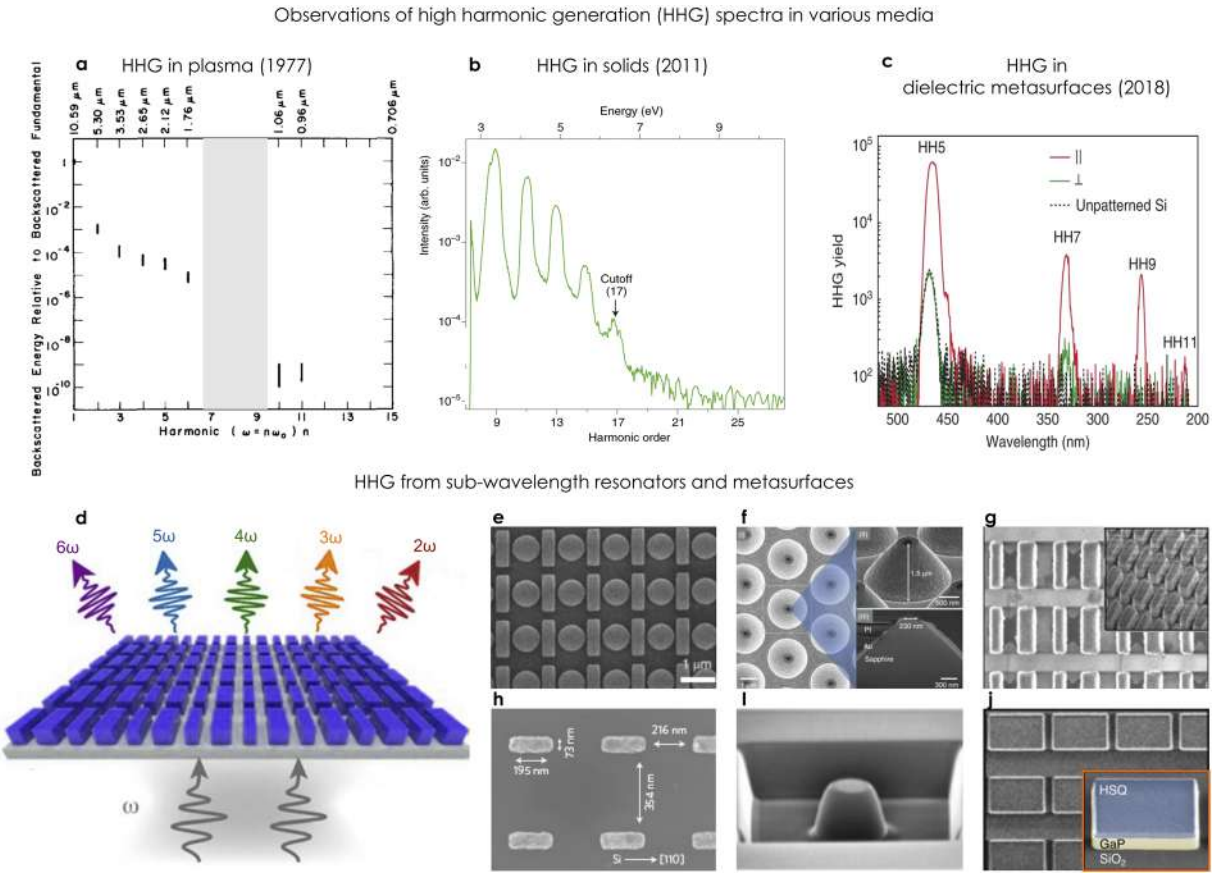

FIG. 4. Generation of high optical harmonics. (a)–(c) observations of high harmonics in (a) plasma, (b) bulk solid state crystals, and (c) in judiciously designed arrays of all-dielectric subwavelength resonators (metasurfaces). (d) Concept image of a metasurface producing multiple optical harmonics. (e)–(j) Examples of subwavelength metal–dielectric and all-dielectric systems for high-harmonic generation. (a) Adapted with permission from Burnett *et al.*, Appl. Phys. Lett. **31**, 172–174 (1977). Copyright 1977 AIP Publishing LLC;[107] (b) Ghimire *et al.*, Nat. Phys. **7**, 138–141 (2011). Copyright 2011 Springer Nature;[115] (c) and (e) Liu *et al.*, Nat. Phys. **14**, 1006–1010 (2018). Copyright 2018 Springer Nature;[121] (f) Han *et al.*, Nat. Commun. **7**, 013105 (2016). Copyright 2016 NLM;[122] (g) Zograf *et al.*, arXiv:2008.11481 (2020). Copyright 2020 Authors CC BY;[123] (h) Vampa *et al.*, Nat. Phys. **13**, 659–662 (2017). Copyright 2017 Springer Nature;[124] (i) Franz *et al.*, Sci. Rep. **9**, 5663 (2019). Copyright 2019 Springer Nature;[125] and (j) Shcherbakov *et al.*, arXiv:2008.03619 (2020). Copyright 2020 Authors CC BY.[126]

such as GaP, enabled the generation of both even and odd high harmonics in transparent metasurfaces over the entire visible range.[126] Even-order optical harmonics up to sixth order and odd harmonics up to ninth order have been observed. Importantly, to avoid laser-induced damage and utilize ultrahigh power excitation, single-shot experiments have enabled a unique physical regime, where the electrons acquire enough momentum to cross the Brillouin zone edges and engage in highly nonlinear Bloch oscillations.[128]

HHG generation at the subwavelength scale differs substantially from HHG in bulk solids. The formation of electron–hole plasma can significantly alter the optical properties of the material during the interaction, which, in turn, changes the optical properties of subwavelength structures. In particular, the resonant wavelength and Q-factor, among other parameters, become dynamically dependent on the optical excitation regimes and nonlinear light–matter interactions. We would expect to see a development of new design principles for non-perturbative nonlinearities that would take into account dynamic changes in the index of refraction and absorption occurring on ultrafast time scales.[86,129]

At present, non-perturbative nonlinear processes at the nanoscale require a self-sufficient ansatz that includes both the non-perturbative response of the underlying materials and the field-dependent resonant properties of the nanostructures. Research on lower-order perturbative nonlinearities at the nanoscale rests on extensive developments of the past covered in multiple reviews.[7,89,130–132] One of the first steps toward bridging the gap between perturbative and non-perturbative nonlinearities at the nanoscale was attempted by Zograf *et al.* in Ref. 123. In that study, researchers merged together two approaches: design principles of BIC metasurfaces,[66] used successfully for perturbative nonlinear optics,[68] with the Keldysh model of free-carrier generation accounting for tunneling and multiphoton absorption processes,[133] used in the past for non-perturbative nonlinear optics. Calculations of field enhancements via the BIC mechanism together

with calculations of plasma-hole density generated in resonant hot spots via non-perturbative light–matter interactions led to a successful description of experimentally observed processes of generation of optical harmonics transitioning from perturbative to non-perturbative regimes.

Illuminating resonant nanostructures with pulse trains at intensities that drive non-perturbative processes may result in unwanted effects such as temperature and free-carrier plasma buildup, as well as multi-pulse laser damage.[134] In order to study the responses of nanostructures bypassing the side effects of pulse trains, in Ref. 126, a single-pulse excitation scheme has been employed. The metasurface was driven into the regime where the Bloch frequency, $\omega_B = eEa/\hbar$ (e is the elementary charge, E is the electric field strength in the metasurface, a is the crystal lattice period, and $\hbar$ is the reduced Planck's constant), has reached the values exceeding the pump frequency by a factor of four, therefore enabling a transition between the perturbative and non-perturbative regimes of harmonic generation.

V. TIME-VARIANT METASURFACES

As shown above, metasurfaces have provided unique ways of controlling the flow of light by employing spatial arrangements of resonant subwavelength particles of designer shapes. The optical properties of metasurfaces are governed by a three-dimensional distribution of the complex refractive index $\tilde{n}(\mathbf{r})$, which often can be considered static. However, this constraint has been recently lifted by time-variant metamaterials and metasurfaces, whereby temporal modulations of the metamaterial's refractive index $\tilde{n}(\mathbf{r}, t)$ can expand the physics of their optical response and offers novel functionalities. Here, we analyze the recent reports that utilize the temporal dimension to control the frequency and propagation flow of light and outline the potential directions of this exciting area of metaphotonics.

Spatiotemporal light control with metamaterials and metasurfaces[135,136] has attracted a lot of attention through extending the versatility of light wave control in metasurfaces to the temporal

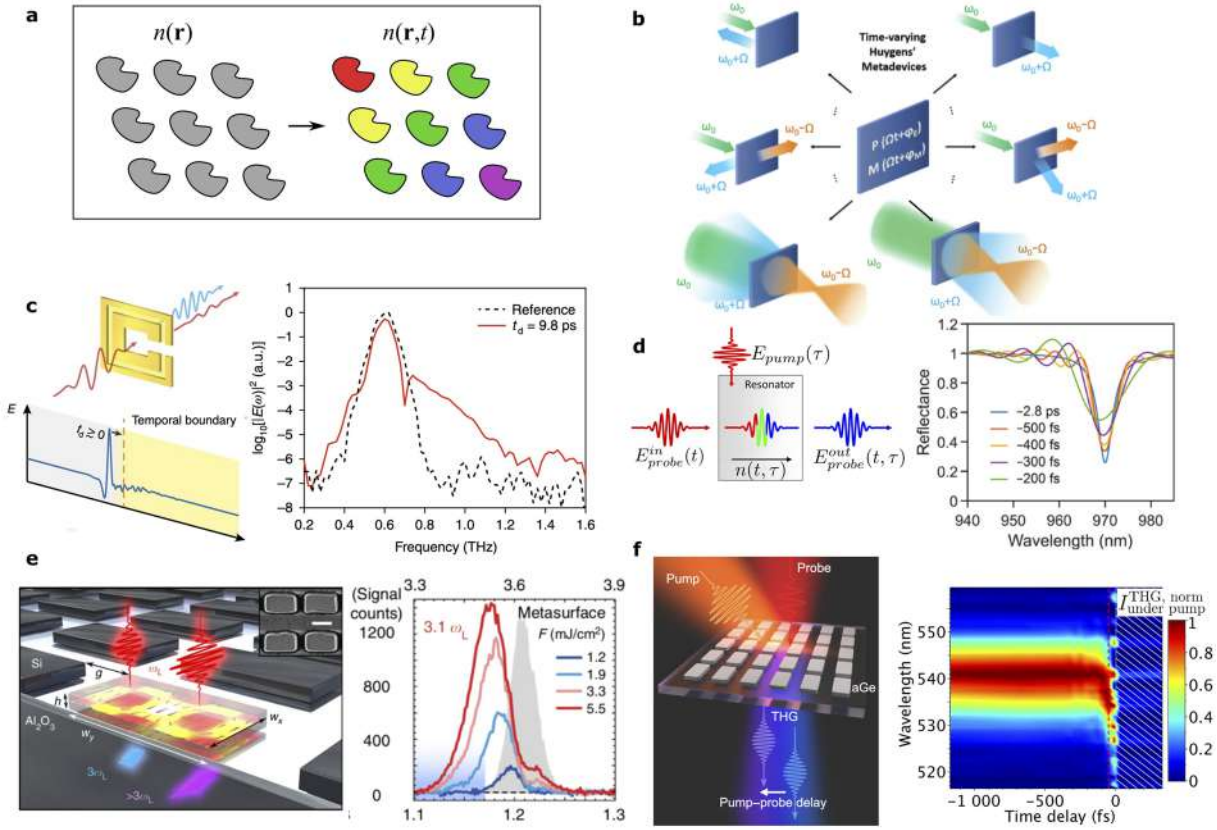

FIG. 5. Time-variant metamaterials enable frequency conversion beyond parametric frequency mixing. (a) The concept of four-dimensional metamaterials. The optical response of a time-variant metamaterial is defined by both the spatial and temporal dependences of the constituent materials' refractive indices. (b) The concept of time-variant Huygens' metadevices.[137] The periodic modulation of both electric and magnetic polarizabilities of the metasurface allows spatiotemporal effects for sideband frequencies. (c) Linear frequency conversion of THz radiation in a time-variant metasurface with a step-like temporal boundary.[138] Being driven at 0.6 THz, the metasurface creates radiation at new frequencies at as high as 1.2 THz due to time-dependent conductivity. (d) Time-variant semiconductor metasurfaces enable frequency conversion in the near-infrared, with transmittance being greater than unity for certain spectral bands.[139] (e) Silicon-based metasurfaces driven by strong mid-infrared femtosecond pulses show photon acceleration, i.e., self-frequency shift, in the third-harmonic response, whereby the central frequency of the THG radiation can be as high as 3.1ω.[140] (f) Frequency conversion of the third-harmonic response in a time-variant germanium metasurface.[141]

dimension. Figure 5(a) outlines this idea: in a conventional metamaterial, the unusual optical properties are achieved via a judiciously chosen distribution of the refractive index $\tilde{n}(\mathbf{r})$ in space. In a time-variant metamaterial, an additional degree of freedom is added by controlling the refractive index as both functions of space and time : $\tilde{n}(\mathbf{r}, t)$. Being spatially inhomogeneous, metasurfaces can alter amplitude, phase, polarization, and angular momenta of light, leading to scattering, diffraction, and spatial mode mixing. Analogously, in a temporally inhomogeneous metamaterial, *frequency modes* can be mixed, whereby the harmonic function in the form of $\mathbf{E}(\mathbf{r}, t) = \mathbf{E}(\mathbf{r})e^{-i\omega t}$ is no longer a solution of Maxwell's equations. Marrying the spatial refractive index engineering with nanotechnology and the temporal refractive index engineering via nonlinear light–matter interactions opens new approaches to demonstrate various effects in photonics using time-variant metasurfaces, such as frequency conversion and nonreciprocal propagation at the nanoscale.

A. Frequency conversion in time-variant metasurfaces

A parametrically modulated electromagnetic system can act as a frequency mixer.[142] The simplest examples include radio-frequency circuits with parametrically changing elements and FM radio. In nonlinear optics, examples of phenomena induced by parametric modulation include sideband generation through Raman or Brillouin scattering.[143] In metasurfaces, two distinct approaches to time modulations can be identified: harmonic modulation and step-like modulation. While the first approach can provide a wider range of accessible frequency detunings, the second approach is generally more efficient in transferring energy between frequency modes. These approaches provide different outlooks on the range of attainable frequency, which, in both cases, is approximately determined by the Fourier spectrum of the parametrically driving stimulus.

Usually, the harmonic modulation of the material's parameters is achieved via a high-frequency electrical drive. Harmonically modulated metasurfaces have been demonstrated in a wide spectral range, from radio frequencies,[137] THz[138] to near-infrared.[144] Figure 5(b) conceptualizes the idea of a harmonically driven metasurface that generates frequency sidebands at $\omega \pm \Omega$, where ω is the free-space radiation frequency and Ω is the driving frequency. Here, the metasurface is engineered to perform various operations on the sideband radiation, including spatial discrimination, lensing, and other operations associated with metasurfaces. The authors showed a variety of frequency-multiplexed functionalities at microwave frequencies using varactor diodes as tunable elements. A potential application based on these effects is a compact beam deflector that could steer one or more generated sidebands at different directions and scan them over the full 4π solid angle. This functionality could benefit the development of new compact radar systems for full-angle and multitarget detection.

A step-like perturbation of the metasurface's refractive index can be achieved through pumping with strong optical pulses. An ultrashort laser pulse rapidly generates free-carrier plasma that can shift the center frequency of a resonator by an amount proportional to the Drude term in the permittivity of the plasma,

$$\Delta\tilde{n}(t) = -\frac{1}{2\tilde{n}}\frac{\omega_p^2(t)}{\omega^2 + i\gamma_c\omega},$$

where $\tilde{n}$ is the static, unperturbed refractive index of the material; $\omega_p(t) = \sqrt{N(t)e^2/\varepsilon_0 m^*}$ is the plasma frequency; and γ_c is the inverse collision time. Here, $\Delta\tilde{n}(t)$ represents dynamic modifications of both the refractive index of a material and its absorption coefficient. First demonstrations of frequency conversion in rapidly generated gaseous plasmas date back to the 1970s and 1980s;[145,146] however, ultrahigh power laser radiation was needed to generate sufficiently dense plasma. It has recently been established that metasurfaces can provide a platform for frequency conversion in semiconductor plasmas at orders-of-magnitude less intensities, making it possible to create frequency converters on a chip. Frequency conversion due to step-like modulation of the refractive index has been reported in THz[138,147] and infrared[139–141] spectral ranges.

The process of frequency conversion in time-variant metasurfaces with a single optical mode can be described using temporal coupled-mode theory,[148]

$$\dot{a}(t) + [i\omega(t) + \gamma_d(t)]a = \sqrt{\kappa}s_+(t),$$

where $a(t)$ is the amplitude of the metasurface's mode, $\omega(t)$ is the time-variant eigenfrequency of the mode, $\gamma_d(t)$ is the time-variant damping factor, $s_+(t)$ is the external excitation, and κ is its coupling constant to the metasurface's mode. If $\omega(t)$ and $\gamma_d(t)$ can be externally controlled by either high-frequency electrical drive or an optical pump, the emitted radiation, given, for instance, by $s_-(t) = s_+(t) - \sqrt{\kappa}a(t)$, can contain frequency components that have not been present in the initial excitation. A general experimental setup for demonstrating the frequency conversion effects in time-variant metasurfaces triggered by an optical pump is given in Fig. 5(d). Here, the probe pulse $E^{in}_{probe}(t) \propto s_+(t)$ is exciting the mode of the metasurface before the pump $E_{\text{pump}}(\tau)$ comes at a time $\tau > t$. The pump imposes a certain step-like dynamics onto $\omega(t)$ and $\gamma(t)$; the result is monitored by measuring the normalized spectrum of the output pulse $T(\omega) = \text{FT}\left|E^{out}_{probe}(t)/E^{in}_{probe}(t)\right|^2$, where FT denotes the Fourier transform. A typical spectrum output from a GaAs metasurface driven by femtosecond pulses[139] is shown in Fig. 5(d). Here, it can be seen that $T(\omega) > 1$ at certain frequencies, denoting frequency conversion due to time modulation, which was also verified in metasurfaces based on amorphous germanium.[149]

VI. CONCLUSIONS AND OUTLOOK

Dielectric nonlinear metasurfaces constitute a rapidly developing field of research driven by the advancements in the design and nanofabrication of subwavelength optical resonators. In this Research Update, we provided a brief overview of strategies and future directions of nonlinear light–matter interactions in dielectric metasurfaces.

We surveyed various analytical approaches in designing resonant nanostructures via composite resonances, including anapole modes, Fano resonances, and bound states in the continuum. As a general trend, the research pursued an increase in the Q-factor of the optical modes at play for boosting the efficiency of the nonlinear interactions in nanoresonators and metasurfaces. A remarkable recent achievement enabled by careful engineering of high-Q modes was the demonstration of a nonlinear optical process in a metasurface under continuous-wave excitation. This is in striking

contrast to common experimental approaches employing short-pulse, high peak power laser sources. Nonlinear nanophotonics in the CW regime of moderate light intensities enabled by recent and ongoing efficiency enhancements in high-Q metasurfaces bear promise for both fundamental and applied research.

We discussed the perspectives of employing machine learning to facilitate further advancements of nonlinear metasurfaces. The progress of machine learning applications to photonics will lead to the rigorous prediction of the nonlinear response, where every aspect of the complex process of nonlinear light–matter interactions can be taken into account. This could facilitate substantially further developments of nonlinear metasurfaces and open up an avenue of opportunities for advanced nonlinear metasurface designs and functionalities.

We reviewed several emerging research directions facilitated by the advancements of dielectric nonlinear metasurfaces. Ultra-strong optical fields coupled with resonant nanostructures provide exciting new opportunities for efficient high-harmonic generation and non-perturbative light–matter interactions at the nanoscale. We expect to see developments in the fundamental understanding of non-perturbative nonlinear processes and, in particular, HHG in dielectric and semiconductor structures engineered on the subwavelength scale. We further expect to see the development of applied aspects of nanoscale HHG toward the miniaturization of novel light sources, such as extreme-UV and attosecond pulse lasers.

We concluded our Research Update by surveying effects in time-variant metasurfaces, an important extension of exiting capabilities of dielectric metasurfaces to control the frequency of light. While frequency conversion in time-variant metamaterials has seen tremendous interest in the past couple of years, there are other exciting directions where the temporally driven meta-atoms can shine. One of them is in creating nonreciprocal devices,[144,150,151] which utilizes the Lorentz reciprocity breaking. The exotic cases of radio-frequency camouflage have been enabled by quasirandom temporal modulation.[152] The possibility of information encoding in orbital angular momentum degrees of freedom has been enabled.[153,154] One of the fundamental tenets of electromagnetic resonators, the time-bandwidth limit, has been challenged in resonators with time-variant parameters.[86,155] Finally, a plethora of effects related to Floquet-type temporal Hamiltonians, traditionally associated with topological photonics,[156] can utilize the synthetic frequency dimension in time-variant resonators,[157] opening avenues for novel topological systems based on time-variant metasurfaces.

We believe that the nascent field of strong-field effects in dielectric metasurfaces can provide unique conditions and materials with tailored nonlinear responses,[158] seeking applications in novel compact light sources and all-optical telecommunications.

AUTHOR'S CONTRIBUTIONS

All authors contributed equally to this work.

ACKNOWLEDGMENTS

The authors are indebted to Professor Yuri Kivshar and Professor Ilya Shadrivov for useful discussions. S.K. acknowledges the Alexander von Humboldt Foundation for financial support. L.C. acknowledges financial support from the European Commission Horizon 2020 H2020-FETOPEN-2018-2020 through Grant Agreement No. 899673 (METAFAST), the National Research Council Joint Laboratories program through Project No. SAC.AD002.026 (OMEN), and the Italian Ministry of University and Research (MIUR) through the PRIN project NOMEN (No. 2017MP7F8F). V.Z. acknowledges financial support from the Ministry of Science and Higher Education of the Russian Federation (No. 14.W03.31.0008) and the MSU Quantum Technology Centre. M.S. and V.Z. acknowledge support from the Russian Science Foundation (No. 18-12-00475).

DATA AVAILABILITY

Data sharing is not applicable to this article as no new data were created or analyzed in this study.

REFERENCES

[1]M. Kauranen and A. V. Zayats, "Nonlinear plasmonics," Nat. Photonics **6**, 737–748 (2012).
[2]N. Meinzer, W. L. Barnes, and I. R. Hooper, "Plasmonic meta-atoms and metasurfaces," Nat. Photonics **8**, 889–898 (2014).
[3]M. A. Garcia, "Surface plasmons in metallic nanoparticles: Fundamentals and applications," J. Phys. D: Appl. Phys. **44**, 283001 (2011).
[4]O. Reshef, M. Saad-Bin-Alam, M. J. Huttunen, G. Carlow, B. T. Sullivan, J.-M. Ménard, K. Dolgaleva, and R. W. Boyd, "Multiresonant high-Q plasmonic metasurfaces," Nano Lett. **19**, 6429–6434 (2019).
[5]H. Aouani, M. Rahmani, M. Navarro-Cía, and S. A. Maier, "Third-harmonic-upconversion enhancement from a single semiconductor nanoparticle coupled to a plasmonic antenna," Nat. Nanotechnol. **9**, 290–294 (2014).
[6]M. Celebrano, X. Wu, M. Baselli, S. Großmann, P. Biagioni, A. Locatelli, C. De Angelis, G. Cerullo, R. Osellame, B. Hecht, L. Duò, F. Ciccacci, and M. Finazzi, "Mode matching in multiresonant plasmonic nanoantennas for enhanced second harmonic generation," Nat. Nanotechnol. **10**, 412–417 (2015).
[7]S. Kruk and Y. Kivshar, "Functional meta-optics and nanophotonics govern by Mie resonances," ACS Photonics **4**, 2638–2649 (2017).
[8]M. I. Shalaev, J. Sun, A. Tsukernik, A. Pandey, K. Nikolskiy, and N. M. Litchinitser, "High-efficiency all-dielectric metasurfaces for ultracompact beam manipulation in transmission mode," Nano Lett. **15**, 6261–6266 (2015).
[9]M. K. Kroychuk, A. S. Shorokhov, D. F. Yagudin, D. A. Shilkin, D. A. Smirnova, I. Volkovskaya, M. R. Shcherbakov, G. Shvets, and A. A. Fedyanin, "Enhanced nonlinear light generation in oligomers of silicon nanoparticles under vector beam illumination," Nano Lett. **20**, 3471–3477 (2020).
[10]E. A. Gurvitz, K. S. Ladutenko, P. A. Dergachev, A. B. Evlyukhin, A. E. Miroshnichenko, and A. S. Shalin, "The high-order toroidal moments and anapole states in all-dielectric photonics," Laser Photonics Rev. **13**, 1800266 (2019).
[11]L. Wang, S. Kruk, K. Koshelev, I. Kravchenko, B. Luther-Davies, and Y. Kivshar, "Nonlinear wavefront control with all-dielectric metasurfaces," Nano Lett. **18**, 3978–3984 (2018).
[12]G. Grinblat, Y. Li, M. P. Nielsen, R. F. Oulton, and S. A. Maier, "Enhanced third harmonic generation in single germanium nanodisks excited at the anapole mode," Nano Lett. **16**, 4635–4640 (2016).
[13]J. Leuthold, C. Koos, and W. Freude, "Nonlinear silicon photonics," Nat. Photonics **4**, 535–544 (2010).
[14]K. Koshelev, S. Kruk, E. Melik-Gaykazyan, J.-H. Choi, A. Bogdanov, H.-G. Park, and Y. Kivshar, "Subwavelength dielectric resonators for nonlinear nanophotonics," Science **367**, 288–292 (2020).
[15]S. Liu, M. B. Sinclair, S. Saravi, G. A. Keeler, Y. Yang, J. Reno, G. M. Peake, F. Setzpfandt, I. Staude, T. Pertsch, and I. Brener, "Resonantly enhanced second-harmonic generation using III–V semiconductor all-dielectric metasurfaces," Nano Lett. **16**, 5426–5432 (2016).
[16]V. F. Gili, L. Carletti, A. Locatelli, D. Rocco, M. Finazzi, L. Ghirardini, I. Favero, C. Gomez, A. Lemaître, M. Celebrano, C. De Angelis, and G. Leo, "Monolithic

AlGaAs second-harmonic nanoantennas," Opt. Express **24**, 15965–15971 (2016).
[17]F. Timpu, J. Sendra, C. Renaut, L. Lang, M. Timofeeva, M. T. Buscaglia, V. Buscaglia, and R. Grange, "Lithium niobate nanocubes as linear and nonlinear ultraviolet Mie resonators," ACS Photonics **6**, 545–552 (2019).
[18]A. Fedotova, M. Younesi, J. Sautter, M. Steinert, R. Geiss, T. Pertsch, I. Staude, and F. Setzpfandt, "Second-harmonic generation in lithium niobate metasurfaces," in *2019 Conference on Lasers and Electro-Optics Europe and European Quantum Electronics Conference* (OSA, 2019), p. ef_1_2.
[19]L. Carletti, A. Zilli, F. Moia, A. Toma, M. Finazzi, C. De Angelis, D. N. Neshev, and M. Celebrano, "Steering and encoding the polarization of the second harmonic in the visible with a monolithic $LiNbO_3$ metasurface," ACS Photonics **8**, 731–737 (2021).
[20]M. Semmlinger, M. Zhang, M. L. Tseng, T.-T. Huang, J. Yang, D. P. Tsai, P. Nordlander, and N. J. Halas, "Generating third harmonic vacuum ultraviolet light with a TiO_2 metasurface," Nano Lett. **19**, 8972–8978 (2019).
[21]F. Timpu, M. Reig Escalé, M. Timofeeva, N. Strkalj, M. Trassin, M. Fiebig, and R. Grange, "Enhanced nonlinear yield from barium titanate metasurface down to the near ultraviolet," Adv. Opt. Mater. **7**, 1900936 (2019).
[22]J. Deng, Y. Tang, S. Chen, K. Li, A. V. Zayats, and G. Li, "Giant enhancement of second-order nonlinearity of epsilon-near-zero medium by a plasmonic metasurface," Nano Lett. **20**, 5421–5427 (2020).
[23]K. Manukyan, M. Z. Alam, C. Liu, K. Pang, H. Song, Z. Zhao, M. Tur, R. W. Boyd, and A. E. Willner, "Interaction between a nanoantenna array and an epsilon-near-zero thin film: Ultrastrong coupling and resonance pinning for engineered highly nonlinear metasurface," in *2020 Conference on Lasers and Electro-Optics (CLEO)* (IEEE, 2020), pp. 1–2.
[24]O. Reshef, I. De Leon, M. Z. Alam, and R. W. Boyd, "Nonlinear optical effects in epsilon-near-zero media," Nat. Rev. Mater. **4**, 535–551 (2019).
[25]F. Yue, R. Piccoli, M. Y. Shalaginov, T. Gu, K. A. Richardson, R. Morandotti, J. Hu, and L. Razzari, "Nonlinear mid-infrared metasurface based on a phase-change material," Laser Photonics Rev. **15**, 2000373 (2021).
[26]N. Bernhardt, K. Koshelev, S. J. U. White, K. W. C. Meng, J. E. Fröch, S. Kim, T. T. Tran, D.-Y. Choi, Y. Kivshar, and A. S. Solntsev, "Quasi-BIC resonant enhancement of second-harmonic generation in WS_2 monolayers," Nano Lett. **20**, 5309–5314 (2020).
[27]Q. Yuan, L. Fang, H. Fang, J. Li, T. Wang, W. Jie, J. Zhao, and X. Gan, "Second harmonic and sum-frequency generations from a silicon metasurface integrated with a two-dimensional material," ACS Photonics **6**, 2252–2259 (2019).
[28]R. Sarma, J. Xu, D. de Ceglia, N. Nookala, L. Carletti, S. Campione, J. Klem, S. D. Gennaro, M. B. Sinclair, M. A. Belkin, and I. Brener, "All-dielectric intersubband polaritonic metasurface with giant second-order nonlinear response," in *Conference on Lasers and Electro-Optics* (OSA, 2020), p. JM1G.4.
[29]A. Mekawy and A. Alù, "Giant midinfrared nonlinearity based on multiple quantum well polaritonic metasurfaces," Nanophotonics **10**, 667–678 (2021).
[30]S. Rubin and Y. Fainman, "Nonlinear, tunable, and active optical metasurface with liquid film," Adv. Photonics **1**, 066003 (2019).
[31]T. Pertsch and Y. Kivshar, "Nonlinear optics with resonant metasurfaces," MRS Bull. **45**, 210–220 (2020).
[32]C. Zou, J. Sautter, F. Setzpfandt, and I. Staude, "Resonant dielectric metasurfaces: Active tuning and nonlinear effects," J. Phys. D: Appl. Phys. **52**, 373002 (2019).
[33]G. Mie, "Beiträge zur Optik trüber Medien, speziell kolloidaler Metallösungen," Ann. Phys. **330**, 377–445 (1908).
[34]C. F. Bohren and D. R. Huffman, *Absorption and Scattering of Light by Small Particles* (Wiley, 1983).
[35]A. I. Kuznetsov, A. E. Miroshnichenko, M. L. Brongersma, Y. S. Kivshar, and B. Luk'yanchuk, "Optically resonant dielectric nanostructures," Science **354**, aag2472 (2016).
[36]I. Staude and J. Schilling, "Metamaterial-inspired silicon nanophotonics," Nat. Photonics **11**, 274–284 (2017).
[37]R. Camacho-Morales, M. Rahmani, S. Kruk, L. Wang, L. Xu, D. A. Smirnova, A. S. Solntsev, A. Miroshnichenko, H. H. Tan, F. Karouta, S. Naureen, K. Vora, L. Carletti, C. De Angelis, C. Jagadish, Y. S. Kivshar, and D. N. Neshev, "Nonlinear generation of vector beams from AlGaAs nanoantennas," Nano Lett. **16**, 7191–7197 (2016).
[38]M. R. Shcherbakov, D. N. Neshev, B. Hopkins, A. S. Shorokhov, I. Staude, E. V. Melik-Gaykazyan, M. Decker, A. A. Ezhov, A. E. Miroshnichenko, I. Brener, A. A. Fedyanin, and Y. S. Kivshar, "Enhanced third-harmonic generation in silicon nanoparticles driven by magnetic response," Nano Lett. **14**, 6488–6492 (2014).
[39]K. Marinov, A. D. Boardman, V. A. Fedotov, and N. Zheludev, "Toroidal metamaterial," New J. Phys. **9**, 324 (2007).
[40]V. Savinov, V. A. Fedotov, and N. I. Zheludev, "Toroidal dipolar excitation and macroscopic electromagnetic properties of metamaterials," Phys. Rev. B: Condens. Matter Mater. Phys. **89**, 205112 (2014).
[41]T. Kaelberer, V. A. Fedotov, N. Papasimakis, D. P. Tsai, and N. I. Zheludev, "Toroidal dipolar response in a metamaterial," Science **330**, 1510–1512 (2010).
[42]V. R. Tuz, V. V. Khardikov, and Y. S. Kivshar, "All-dielectric resonant metasurfaces with a strong toroidal response," ACS Photonics **5**, 1871–1876 (2018).
[43]G. Zhang, C. Lan, R. Gao, Y. Wen, and J. Zhou, "Toroidal dipole resonances in all-dielectric oligomer metasurfaces," Adv. Theory Simul. **2**, 1900123 (2019).
[44]X. Luo, X. Li, T. Lang, X. Jing, and Z. Hong, "Excitation of high Q toroidal dipole resonance in an all-dielectric metasurface," Opt. Mater. Express **10**, 358–368 (2020).
[45]C. Cui, S. Yuan, X. Qiu, L. Zhu, Y. Wang, Y. Li, J. Song, Q. Huang, C. Zeng, and J. Xia, "Light emission driven by magnetic and electric toroidal dipole resonances in a silicon metasurface," Nanoscale **11**, 14446–14454 (2019).
[46]J. Jeong, M. D. Goldflam, S. Campione, J. L. Briscoe, P. P. Vabishchevich, J. Nogan, M. B. Sinclair, T. S. Luk, and I. Brener, "High quality factor toroidal resonances in dielectric metasurfaces," ACS Photonics **7**, 1699–1707 (2020).
[47]A. Ahmadivand, M. Semmlinger, L. Dong, B. Gerislioglu, P. Nordlander, and N. J. Halas, "Toroidal dipole-enhanced third harmonic generation of deep ultraviolet light using plasmonic meta-atoms," Nano Lett. **19**, 605–611 (2019).
[48]A. E. Miroshnichenko, A. B. Evlyukhin, Y. F. Yu, R. M. Bakker, A. Chipouline, A. I. Kuznetsov, B. Luk'yanchuk, B. N. Chichkov, and Y. S. Kivshar, "Nonradiating anapole modes in dielectric nanoparticles," Nat. Commun. **6**, 8069 (2015).
[49]L. Xu, M. Rahmani, K. Zangeneh Kamali, A. Lamprianidis, L. Ghirardini, J. Sautter, R. Camacho-Morales, H. Chen, M. Parry, I. Staude, G. Zhang, D. Neshev, and A. E. Miroshnichenko, "Boosting third-harmonic generation by a mirror-enhanced anapole resonator," Light Sci. Appl. **7**, 44 (2018).
[50]G. Grinblat, Y. Li, M. P. Nielsen, R. F. Oulton, and S. A. Maier, "Efficient third harmonic generation and nonlinear subwavelength imaging at a higher-order anapole mode in a single germanium nanodisk," ACS Nano **11**, 953–960 (2017).
[51]J. Jin, X. Yin, L. Ni, M. Soljačić, B. Zhen, and C. Peng, "Topologically enabled ultrahigh-Q guided resonances robust to out-of-plane scattering," Nature **574**, 501–504 (2019).
[52]T. Zhang, Y. Che, K. Chen, J. Xu, Y. Xu, T. Wen, G. Lu, X. Liu, B. Wang, X. Xu, Y. S. Duh, Y. L. Tang, J. Han, Y. Cao, B. O. Guan, S. W. Chu, and X. Li, "Anapole mediated giant photothermal nonlinearity in nanostructured silicon," Nat. Commun. **11**, 3027 (2020).
[53]T. Shibanuma, G. Grinblat, P. Albella, and S. A. Maier, "Efficient third harmonic generation from metal-dielectric hybrid nanoantennas," Nano Lett. **17**, 2647–2651 (2017).
[54]V. F. Gili, L. Ghirardini, D. Rocco, G. Marino, I. Favero, I. Roland, G. Pellegrini, L. Duò, M. Finazzi, L. Carletti, A. Locatelli, A. Lemaître, D. Neshev, C. De Angelis, G. Leo, and M. Celebrano, "Metal-dielectric hybrid nanoantennas for efficient frequency conversion at the anapole mode," Beilstein J. Nanotechnol. **9**, 2306–2314 (2018).
[55]M. V. Rybin, K. L. Koshelev, Z. F. Sadrieva, K. B. Samusev, A. A. Bogdanov, M. F. Limonov, and Y. S. Kivshar, "High-Q supercavity modes in subwavelength dielectric resonators," Phys. Rev. Lett. **119**, 243901 (2017).
[56]Y. Yang, W. Wang, A. Boulesbaa, I. I. Kravchenko, D. P. Briggs, A. Puretzky, D. Geohegan, and J. Valentine, "Nonlinear Fano-resonant dielectric metasurfaces," Nano Lett. **15**, 7388–7393 (2015).
[57]Z. Liu, Y. Xu, Y. Lin, J. Xiang, T. Feng, Q. Cao, J. Li, S. Lan, and J. Liu, "High-Q quasibound states in the continuum for nonlinear metasurfaces," Phys. Rev. Lett. **123**, 253901 (2019).

[58] A. P. Anthur, H. Zhang, R. Paniagua-Dominguez, D. A. Kalashnikov, S. T. Ha, T. W. W. Maß, A. I. Kuznetsov, and L. Krivitsky, "Continuous wave second harmonic generation enabled by quasi-bound-states in the continuum on gallium phosphide metasurfaces," Nano Lett. **20**, 8745–8751 (2020).
[59] K. Koshelev, A. Bogdanov, and Y. Kivshar, "Meta-optics and bound states in the continuum," Sci. Bull. **64**, 836–842 (2019).
[60] H. Friedrich and D. Wintgen, "Interfering resonances and bound states in the continuum," Phys. Rev. A **32**, 3231 (1985).
[61] L. Carletti, S. S. Kruk, A. A. Bogdanov, C. De Angelis, and Y. Kivshar, "High-harmonic generation at the nanoscale boosted by bound states in the continuum," Phys. Rev. Res. **1**, 023016 (2019).
[62] L. Carletti, K. Koshelev, C. De Angelis, and Y. Kivshar, "Giant nonlinear response at the nanoscale driven by bound states in the continuum," Phys. Rev. Lett. **121**, 033903 (2018).
[63] E. Melik-gaykazyan, K. Koshelev, J.-H. Choi, S. S. Kruk, A. Bogdanov, H.-G. Park, and Y. Kivshar, "From Fano to quasi-BIC resonances in individual dielectric nanoantennas," Nano Lett. **21**, 1765–1771 (2021).
[64] B. Luk'Yanchuk, N. I. Zheludev, S. A. Maier, N. J. Halas, P. Nordlander, H. Giessen, and C. T. Chong, "The Fano resonance in plasmonic nanostructures and metamaterials," Nat. Mater. **9**, 707–715 (2010).
[65] M. F. Limonov, M. V. Rybin, A. N. Poddubny, and Y. S. Kivshar, "Fano resonances in photonics," Nat. Photonics **11**, 543–554 (2017).
[66] K. Koshelev, S. Lepeshov, M. Liu, A. Bogdanov, and Y. Kivshar, "Asymmetric metasurfaces with high-Q resonances governed by bound states in the continuum," Phys. Rev. Lett. **121**, 193903 (2018).
[67] P. P. Vabishchevich, S. Liu, M. B. Sinclair, G. A. Keeler, G. M. Peake, and I. Brener, "Enhanced second-harmonic generation using broken symmetry III–V semiconductor Fano metasurfaces," ACS Photonics **5**, 1685–1690 (2018).
[68] K. Koshelev, Y. Tang, K. Li, D.-Y. Choi, G. Li, and Y. Kivshar, "Nonlinear metasurfaces governed by bound states in the continuum," ACS Photonics **6**, 1639–1644 (2019).
[69] S. Jafar-Zanjani, S. Inampudi, and H. Mosallaei, "Adaptive genetic algorithm for optical metasurfaces design," Sci. Rep. **8**, 11040 (2018).
[70] H. Yang, X. Cao, F. Yang, J. Gao, S. Xu, M. Li, X. Chen, Y. Zhao, Y. Zheng, and S. Li, "A programmable metasurface with dynamic polarization, scattering and focusing control," Sci. Rep. **6**, 35692 (2016).
[71] M. M. R. Elsawy, S. Lanteri, R. Duvigneau, J. A. Fan, and P. Genevet, "Numerical optimization methods for metasurfaces," Laser Photonics Rev. **14**, 1900445 (2020).
[72] C. C. Nadell, B. Huang, J. M. Malof, and W. J. Padilla, "Deep learning for accelerated all-dielectric metasurface design," Opt. Express **27**, 27523 (2019).
[73] J. A. Fan, "Optimization and machine learning for metasurface design (conference presentation)," in *High Contrast Metastructures VIII* (SPIE, 2019), Vol. 10928.
[74] I. Malkiel, M. Mrejen, L. Wolf, and H. Suchowski, "Machine learning for nanophotonics," MRS Bull. **45**, 221–229 (2020).
[75] S. An, C. Fowler, B. Zheng, M. Y. Shalaginov, H. Tang, H. Li, L. Zhou, J. Ding, A. M. Agarwal, C. Rivero-Baleine, K. A. Richardson, T. Gu, J. Hu, and H. Zhang, "A deep learning approach for objective-driven all-dielectric metasurface design," ACS Photonics **6**, 3196–3207 (2019).
[76] G. Cybenko, "Approximation by superpositions of a sigmoidal function," Math. Control Signals Syst. **2**, 303–314 (1989).
[77] K. Hornik, M. Stinchcombe, and H. White, "Multilayer feedforward networks are universal approximators," Neural Networks **2**, 359–366 (1989).
[78] K. Hornik, M. Stinchcombe, and H. White, "Universal approximation of an unknown mapping and its derivatives using multilayer feedforward networks," Neural Networks **3**, 551–560 (1990).
[79] J. Peurifoy, Y. Shen, L. Jing, Y. Yang, F. Cano-Renteria, B. G. DeLacy, J. D. Joannopoulos, M. Tegmark, and M. Soljačić, "Nanophotonic particle simulation and inverse design using artificial neural networks," Sci. Adv. **4**, eaar4206 (2018).
[80] Z. Liu, D. Zhu, S. P. Rodrigues, K.-T. Lee, and W. Cai, "Generative model for the inverse design of metasurfaces," Nano Lett. **18**, 6570–6576 (2018).
[81] W. Ma, F. Cheng, and Y. Liu, "Deep-learning-enabled on-demand design of chiral metamaterials," ACS Nano **12**, 6326–6334 (2018).
[82] I. Malkiel, M. Mrejen, A. Nagler, U. Arieli, L. Wolf, and H. Suchowski, "Plasmonic nanostructure design and characterization via Deep Learning," Light Sci. Appl. **7**, 60 (2018).
[83] M. V. Zhelyeznyakov, S. Brunton, and A. Majumdar, "Deep learning to accelerate scatterer-to-field mapping for inverse design of dielectric metasurfaces," ACS Photonics **8**, 481–488 (2021).
[84] L. Jiang, X. Li, Q. Wu, L. Wang, and L. Gao, "Neural network enabled metasurface design for phase manipulation," Opt. Express **29**, 2521–2528 (2021).
[85] B. Frazier, T. Antonsen, and S. Anlage, "Deep learning enabled wavefront shaping in complex cavities with a binary tunable metasurface," Bull. Am. Phys. Soc. **5**, 00003 (2021), available at https://meetings.aps.org/Meeting/MAR21/Session/Y05.3.
[86] M. R. Shcherbakov, P. Shafirin, and G. Shvets, "Overcoming the efficiency-bandwidth tradeoff for optical harmonics generation using nonlinear time-variant resonators," Phys. Rev. A **100**, 063847 (2019).
[87] C. Schlickriede, S. S. Kruk, L. Wang, B. Sain, Y. Kivshar, and T. Zentgraf, "Nonlinear imaging with all-dielectric metasurfaces," Nano Lett. **20**, 4370–4376 (2020).
[88] Y. Gao, Y. Fan, Y. Wang, W. Yang, Q. Song, and S. Xiao, "Nonlinear holographic all-dielectric metasurfaces," Nano Lett. **18**, 8054–8061 (2018).
[89] J. Bar-David and U. Levy, "Nonlinear diffraction in asymmetric dielectric metasurfaces," Nano Lett. **19**, 1044–1051 (2019).
[90] B. Reineke, B. Sain, R. Zhao, L. Carletti, B. Liu, L. Huang, C. De Angelis, and T. Zentgraf, "Silicon metasurfaces for third harmonic geometric phase manipulation and multiplexed holography," Nano Lett. **19**, 6585–6591 (2019).
[91] B. Liu, B. Sain, B. Reineke, R. Zhao, C. Meier, L. Huang, Y. Jiang, and T. Zentgraf, "Nonlinear wavefront control by geometric-phase dielectric metasurfaces: Influence of mode field and rotational symmetry," Adv. Opt. Mater. **8**, 1902050 (2020).
[92] G. Li, S. Chen, N. Pholchai, B. Reineke, P. W. H. Wong, E. Y. B. Pun, K. W. Cheah, T. Zentgraf, and S. Zhang, "Continuous control of the nonlinearity phase for harmonic generations," Nat. Mater. **14**, 607–612 (2015).
[93] M. R. Shcherbakov, P. P. Vabishchevich, A. S. Shorokhov, K. E. Chong, D.-Y. Choi, I. Staude, A. E. Miroshnichenko, D. N. Neshev, A. A. Fedyanin, and Y. S. Kivshar, "Ultrafast all-optical switching with magnetic resonances in nonlinear dielectric nanostructures," Nano Lett. **15**, 6985–6990 (2015).
[94] M. Lawrence, D. R. Barton, and J. A. Dionne, "Nonreciprocal flat optics with silicon metasurfaces," Nano Lett. **18**, 1104–1109 (2018).
[95] S. Kruk, L. Wang, B. Sain, Z. Dong, J. Yang, T. Zentgraf, and Y. Kivshar, "Asymmetric light generation in nonlinear metasurfaces," in *2020 MRS Fall Meeting* (Materials Conference Society, 2020), p. F.NM02.04.31.
[96] E. Almeida, O. Bitton, and Y. Prior, "Nonlinear metamaterials for holography," Nat. Commun. **7**, 12533 (2016).
[97] C. Schlickriede, N. Waterman, B. Reineke, P. Georgi, G. Li, S. Zhang, and T. Zentgraf, "Imaging through nonlinear metalens using second harmonic generation," Adv. Opt. Mater. **30**, 1703843 (2018).
[98] Y. Xu, J. Sun, J. Frantz, M. I. Shalaev, W. Walasik, A. Pandey, J. D. Myers, R. Y. Bekele, A. Tsukernik, J. S. Sanghera, and N. M. Litchinitser, "Reconfiguring structured light beams using nonlinear metasurfaces," Opt. Express **26**, 30930–30943 (2018).
[99] M. R. Shcherbakov, S. Liu, V. V. Zubyuk, A. Vaskin, P. P. Vabishchevich, G. Keeler, T. Pertsch, T. V. Dolgova, I. Staude, I. Brener, and A. A. Fedyanin, "Ultrafast all-optical tuning of direct-gap semiconductor metasurfaces," Nat. Commun. **8**, 17 (2017).
[100] V. V. Zubyuk, P. P. Vabishchevich, M. R. Shcherbakov, A. S. Shorokhov, A. N. Fedotova, S. Liu, G. Keeler, T. V. Dolgova, I. Staude, I. Brener, and A. A. Fedyanin, "Low-power absorption saturation in semiconductor metasurfaces," ACS Photonics **6**, 2797–2806 (2019).
[101] B. Jin and C. Argyropoulos, "Self-induced passive nonreciprocal transmission by nonlinear bifacial dielectric metasurfaces," Phys. Rev. Appl. **13**, 054056 (2020).
[102] L. Cheng, R. Alaee, A. Safari, M. Karimi, L. Zhang, and R. W. Boyd, "Superscattering, superabsorption, and nonreciprocity in nonlinear antennas," ACS Photonics **8**, 585–591 (2021).
[103] M. Z. Alam, I. De Leon, and R. W. Boyd, "Large optical nonlinearity of indium tin oxide in its epsilon-near-zero region," Science **352**, 795–797 (2016).

[104]E. Poutrina and A. Urbas, "Multipolar interference for nonreciprocal nonlinear generation," Sci. Rep. **6**, 25113 (2016).
[105]K.-H. Kim, "Asymmetric second-harmonic generation with high efficiency from a non-chiral hybrid bilayer complementary metasurface," Plasmonics **16**, 77–82 (2021).
[106]N. Shitrit, J. Kim, D. S. Barth, H. Ramezani, Y. Wang, and X. Zhang, "Asymmetric free-space light transport at nonlinear metasurfaces," Phys. Rev. Lett. **121**, 046101 (2018).
[107]N. H. Burnett, H. A. Baldis, M. C. Richardson, and G. D. Enright, "Harmonic generation in CO_2 laser target interaction," Appl. Phys. Lett. **31**, 172–174 (1977).
[108]M. Ferray, A. L'Huillier, X. F. Li, L. A. Lompre, G. Mainfray, and C. Manus, "Multiple-harmonic conversion of 1064 nm radiation in rare gases," J. Phys. B: At. Mol. Opt. Phys. **21**, L31 (1988).
[109]J. L. Krause, K. J. Schafer, and K. C. Kulander, "High-order harmonic generation from atoms and ions in the high intensity regime," Phys. Rev. Lett. **68**, 3535–3538 (1992).
[110]K. J. Schafer, B. Yang, L. F. Dimauro, and K. C. Kulander, "Above threshold ionization beyond the high harmonic cutoff," Phys. Rev. Lett. **70**, 1599–1602 (1993).
[111]H. R. Reiss, "Complete Keldysh theory and its limiting cases," Phys. Rev. A **42**, 1476–1486 (1990).
[112]A. Paul, R. A. Bartels, R. Tobey, H. Green, S. Weiman, I. P. Christov, M. M. Murnane, H. C. Kapteyn, and S. Backus, "Quasi-phase-matched generation of coherent extreme-ultraviolet light," Nature **421**, 51–54 (2003).
[113]A. Baltuška, T. Udem, M. Uiberacker, M. Hentschel, E. Goulielmakis, Ch Gohle, R. Holzwarth, V. S. Yakovlev, A. Scrinzi, T. W. Hänsch, and F. Krausz, "Attosecond control of electronic processes by intense light fields," Nature **421**, 611–615 (2003).
[114]J. Itatani, J. Levesque, D. Zeidler, H. Niikura, H. Pépin, J. C. Kieffer, P. B. Corkum, and D. M. Villeneuve, "Tomographic imaging of molecular orbitals," Nature **432**, 867–871 (2004).
[115]S. Ghimire, A. D. Dichiara, E. Sistrunk, P. Agostini, L. F. Dimauro, and D. A. Reis, "Observation of high-order harmonic generation in a bulk crystal," Nat. Phys. **7**, 138–141 (2011).
[116]S. Ghimire and D. A. Reis, "High-harmonic generation from solids," Nat. Phys. **15**, 10–16 (2019).
[117]Y. Yang, J. Lu, A. Manjavacas, T. S. Luk, H. Liu, K. Kelley, J.-P. Maria, E. L. Runnerstrom, M. B. Sinclair, S. Ghimire, and I. Brener, "High-harmonic generation from an epsilon-near-zero material," Nat. Phys. **15**, 1022–1026 (2019).
[118]N. Yoshikawa, T. Tamaya, and K. Tanaka, "Optics: High-harmonic generation in graphene enhanced by elliptically polarized light excitation," Science **356**, 736–738 (2017).
[119]H. Liu, Y. Li, Y. S. You, S. Ghimire, T. F. Heinz, and D. A. Reis, "High-harmonic generation from an atomically thin semiconductor," Nat. Phys. **13**, 262–265 (2017).
[120]G. Vampa, T. J. Hammond, N. Thiré, B. E. Schmidt, F. Légaré, C. R. McDonald, T. Brabec, and P. B. Corkum, "Linking high harmonics from gases and solids," Nature **522**, 462–464 (2015).
[121]H. Liu, C. Guo, G. Vampa, J. L. Zhang, T. Sarmiento, M. Xiao, P. H. Bucksbaum, J. Vučković, S. Fan, and D. A. Reis, "Enhanced high-harmonic generation from an all-dielectric metasurface," Nat. Phys. **14**, 1006–1010 (2018).
[122]S. Han, H. Kim, Y. W. Kim, Y. J. Kim, S. Kim, I. Y. Park, and S. W. Kim, "High-harmonic generation by field enhanced femtosecond pulses in metal-sapphire nanostructure," Nat. Commun. **7**, 13105 (2016).
[123]G. Zograf, K. Koshelev, A. Zalogina, V. Korolev, D.-Y. Choi, M. Zurch, C. Spielmann, B. Luther-Davies, D. Kartashov, S. Makarov, S. Kruk, and Y. Kivshar, "High-harmonic generation from metasurfaces empowered by bound states in the continuum," arXiv:2008.11481 (2020).
[124]G. Vampa, B. G. Ghamsari, S. Siadat Mousavi, T. J. Hammond, A. Olivieri, E. Lisicka-Skrek, A. Y. Naumov, D. M. Villeneuve, A. Staudte, P. Berini, and P. B. Corkum, "Plasmon-enhanced high-harmonic generation from silicon," Nat. Phys. **13**, 659–662 (2017).
[125]D. Franz, S. Kaassamani, D. Gauthier, R. Nicolas, M. Kholodtsova, L. Douillard, J. T. Gomes, L. Lavoute, D. Gaponov, N. Ducros, S. Février, J. Biegert, L. Shi, M. Kovacev, W. Boutu, and H. Merdji, "All semiconductor enhanced high-harmonic generation from a single nanostructured cone," Sci. Rep. **9**, 5663 (2019).
[126]M. R. Shcherbakov, H. Zhang, M. Tripepi, G. Sartorello, N. Talisa, A. Alshafey, Z. Fan, J. Twardowski, L. A. Krivitsky, A. I. Kuznetsov, E. Chowdhury, and G. Shvets, "Generation of even and odd high harmonics in resonant metasurfaces using single and multiple ultra-intense laser pulses," arXiv:2008.03619 (2020).
[127]H. Liu, G. Vampa, J. L. Zhang, Y. Shi, S. Buddhiraju, S. Fan, J. Vuckovic, P. H. Bucksbaum, and D. A. Reis, "Overcoming the absorption limit in high-harmonic generation from crystals," Commun. Phys. **3**, 192 (2020).
[128]O. Schubert, M. Hohenleutner, F. Langer, B. Urbanek, C. Lange, U. Huttner, D. Golde, T. Meier, M. Kira, S. W. Koch, and R. Huber, "Sub-cycle control of terahertz high-harmonic generation by dynamical Bloch oscillations," Nat. Photonics **8**, 119–123 (2014).
[129]J.-K. An and K.-H. Kim, "Efficient non-perturbative high-harmonic generation from nonlinear metasurfaces with low pump intensity," Opt. Laser Technol. **135**, 106702 (2021).
[130]A. Krasnok, M. Tymchenko, and A. Alù, "Nonlinear metasurfaces: A paradigm shift in nonlinear optics," Mater. Today **21**, 8–21 (2017).
[131]B. Sain, C. Meier, and T. Zentgraf, "Nonlinear optics in all-dielectric nanoantennas and metasurfaces: A review," Adv. Photonics **1**, 024002 (2019).
[132]G. Li, S. Zhang, and T. Zentgraf, "Nonlinear photonic metasurfaces," Nat. Rev. Mater. **2**, 17010 (2017).
[133]P. Balling and J. Schou, "Femtosecond-laser ablation dynamics of dielectrics: Basics and applications for thin films," Rep. Prog. Phys. **76**, 036502 (2013).
[134]M. Mero, "On the damage behavior of dielectric films when illuminated with multiple femtosecond laser pulses," Opt. Eng. **44**, 051107 (2005).
[135]A. M. Shaltout, V. M. Shalaev, and M. L. Brongersma, "Spatiotemporal light control with active metasurfaces," Science **364**, eaat3100 (2019).
[136]M. R. Shcherbakov, F. Eilenberger, and I. Staude, "Interaction of semiconductor metasurfaces with short laser pulses: From nonlinear-optical response toward spatiotemporal shaping," J. Appl. Phys. **126**, 085705 (2019).
[137]M. Liu, D. A. Powell, Y. Zarate, and I. V. Shadrivov, "Huygens' metadevices for parametric waves," Phys. Rev. X **8**, 031077 (2018).
[138]K. Lee, J. Son, J. Park, B. Kang, W. Jeon, F. Rotermund, and B. Min, "Linear frequency conversion via sudden merging of meta-atoms in time-variant metasurfaces," Nat. Photonics **12**, 765–774 (2018).
[139]N. Karl, P. P. Vabishchevich, M. R. Shcherbakov, S. Liu, M. B. Sinclair, G. Shvets, and I. Brener, "Frequency conversion in a time-variant dielectric metasurface," Nano Lett. **20**, 7052–7058 (2020).
[140]M. R. Shcherbakov, K. Werner, Z. Fan, N. Talisa, E. Chowdhury, and G. Shvets, "Photon acceleration and tunable broadband harmonics generation in nonlinear time-dependent metasurfaces," Nat. Commun. **10**, 1345 (2019).
[141]V. V. Zubyuk, P. A. Shafirin, M. R. Shcherbakov, G. Shvets, and A. A. Fedyanin, "Externally driven nonlinear time-variant metasurfaces," arXiv:2012.06604 (2020).
[142]P. K. Tien, "Parametric amplification and frequency mixing in propagating circuits," J. Appl. Phys. **29**, 1347 (1958).
[143]S. L. Shapiro, J. A. Giordmaine, and K. W. Wecht, "Stimulated Raman and Brillouin scattering with picosecond light pulses," Phys. Rev. Lett. **19**, 1093 (1967).
[144]X. Guo, Y. Ding, Y. Duan, and X. Ni, "Nonreciprocal metasurface with space–time phase modulation," Light Sci. Appl. **8**, 123 (2019).
[145]E. Yablonovitch, "Spectral broadening in the light transmitted through a rapidly growing plasma," Phys. Rev. Lett. **31**, 877 (1973).
[146]S. C. Wilks, J. M. Dawson, W. B. Mori, T. Katsouleas, and M. E. Jones, "Photon accelerator," Phys. Rev. Lett. **62**, 2600 (1989).
[147]K. Lee, J. Park, J. Son, B. J. Kang, W. T. Kim, S. C. Lee, B. Min, and F. Rotermund, "Electrical control of terahertz frequency conversion from time-varying surfaces," Opt. Express **27**, 12762–12773 (2019).
[148]S. Fan, W. Suh, and J. D. Joannopoulos, "Temporal coupled-mode theory for the Fano resonance in optical resonators," J. Opt. Soc. Am. A **20**, 569–572 (2003).
[149]M. R. Shcherbakov, R. Lemasters, Z. Fan, J. Song, T. Lian, H. Harutyunyan, and G. Shvets, "Time-variant metasurfaces enable tunable spectral bands of negative extinction," Optica **6**, 1441–1442 (2019).

[150]J. W. Zang, D. Correas-Serrano, J. T. S. Do, X. Liu, A. Alvarez-Melcon, and J. S. Gomez-Diaz, "Nonreciprocal wavefront engineering with time-modulated gradient metasurfaces," Phys. Rev. Appl. **11**, 054054 (2019).
[151]A. E. Cardin, S. R. Silva, S. R. Vardeny, W. J. Padilla, A. Saxena, A. J. Taylor, W. J. M. Kort-Kamp, H. T. Chen, D. A. R. Dalvit, and A. K. Azad, "Surface-wave-assisted nonreciprocity in spatio-temporally modulated metasurfaces," Nat. Commun. **11**, 1469 (2020).
[152]M. Liu, A. B. Kozyrev, and I. V. Shadrivov, "Time-varying metasurfaces for broadband spectral camouflage," Phys. Rev. Appl. **12**, 054052 (2019).
[153]H. Barati Sedeh, M. M. Salary, and H. Mosallaei, "Time-varying optical vortices enabled by time-modulated metasurfaces," Nanophotonics **9**, 2957–2976 (2020).
[154]H. Barati Sedeh, M. M. Salary, and H. Mosallaei, "Topological space-time photonic transitions in angular-momentum-biased metasurfaces," Adv. Opt. Mater. **8**, 2000075 (2020).
[155]Z. Hayran and F. Monticone, "Capturing broadband light in a compact bound state in the continuum," ACS Photonics **8**(3), 813–823 (2021).
[156]M. C. Rechtsman, J. M. Zeuner, Y. Plotnik, Y. Lumer, D. Podolsky, F. Dreisow, S. Nolte, M. Segev, and A. Szameit, "Photonic Floquet topological insulators," Nature **496**, 196–200 (2013).
[157]A. Dutt, Q. Lin, L. Yuan, M. Minkov, M. Xiao, and S. Fan, "A single photonic cavity with two independent physical synthetic dimensions," Science **367**, 59–64 (2020).
[158]M. Ren, W. Cai, and J. Xu, "Tailorable dynamics in nonlinear optical metasurfaces," Adv. Mater. **32**, 1806317 (2020).